Resonant Acoustic Profiling for Biological Detection and Diagnostics

W. Chiu, C.J. Hammond, R. Hammond, L. Harding, E. Hawkins, X. Li, S. Moore, K. Sanders, A. Sleptsov, C. Zhou and M.A. Cooper*

Cambridge Medical Innovations
181 Cambridge Science Park, Cambridge CB4 0GJ, UK
mcooper@cam-medical.com

***Abstract*†— We have employed bulk acoustic wave and surface acoustic wave devices for the sensitive and specific detection of biological agents in complex liquid media. We have produced a robotic liquid delivery system coupled to a multi-layer microfluidic manifold that delivers liquids in a controlled manner to pairs of resonant acoustic sensors in a 'USB' type docking station. These resonators were fabricated on a single wafer of piezoelectric material, and a rapid switching process between active areas employed to eliminate cross talk and interference. System performance was enhanced using a proprietary FPGA-based network analyzer with internal digital synthesizer, RF switches and calibration elements. Before the signal was sent to the sensor interface, the impedance of the signal path was transferred to match the sensor interface impedance. The sensors are coated with proprietary planar surface chemistries and polymeric interfaces optimised for biological compatibility, shear modulus and penetration depth to maximise acoustic coupling of a binding signal to the sensor. An optimised elastomeric mounting was developed to minimise the impact of thermal and motional stress on the piezoelectric material, whilst simultaneously providing a sub-microlitre microfluidic dead volume above the sensor. Herein we demonstrate the utility of the system using analytes at each end of the molecular weight range: small molecular weight drug candidates binding to a protein receptor and high molecular weight bacteria binding to an antibody.**

I. INTRODUCTION

Acoustic biosensors allow the label-free detection of molecules and the analysis of binding events. In general, they are based on quartz crystal resonators, in which the mode of oscillation depends on the cut and geometry of the quartz crystal. If mass is applied on to the surface of the quartz resonator, the frequency of the oscillation decreases. By measuring the change of frequency, it is possible to determine the change in mass. Measurement of mass by using quartz crystal resonators was first examined by Sauerbrey [1], who showed that the frequency change of the crystal resonator is a linear function of the mass per area m_s, or absolute mass Δm :

$$\Delta f_m = -\frac{f_0^2}{F_q \rho_q} m_s = -\frac{f_0^2}{F_q \rho_q} \frac{\Delta m_s}{A_{el}} \tag{1}$$

f_0 is the resonance frequency of the unperturbed quartz resonator, F_q the frequency constant of the crystal ($F_q = f_0.d_q$), d_q the thickness, ρ_q the mass density, and A_{el} the electrode size of the crystal resonator. The above equation is only valid for thin, solid layers deposited on the resonator.

Initially the QCM system was used for dry measurements; later on when suitable oscillator circuits were developed, it was possible to carry out measurements under liquid conditions [2]. This method led to the use of QCM systems as biosensors to detect molecular interactions. A new equation was derived by Kanazawa and Gordon to explain the relationship between density (ρ_l) and viscosity (η_l) of the liquid and the frequency of the quartz crystal resonator:

$$\Delta f = -f_q^{3/2} \sqrt{\frac{\rho_l \eta_l}{\pi \rho_q \mu_q}} \tag{2}$$

where ρ_q and μ_q are the quartz density and shear modulus, respectively [3]. In a two layer system these frequency shifts simplistically (ignoring viscoelastic and complex shear modulus contributions) add up to an overall shift:

$$\Delta f = \Delta f_m + \Delta f_l = -f_0^2 \left(\frac{\Delta m_s}{F_q \rho_q A_{el}} + \sqrt{\frac{\eta_l \rho_l}{f_0 \pi \mu_q \rho_q}} \right) \tag{3}$$

The advantages of acoustic sensor systems that exploit the piezoelectric effect to measure mass binding and molecular

† This work was supported by NIAID Grant U01-AI-061243

interactions have long been discussed, with the technology proffered as an alternative to optical biosensors [4]. The technique has also been shown to be capable of detecting subtle changes in the solution-surface interface that can be due to density-viscosity changes in the solution, viscoelastic changes in the bound interfacial material, and changes in the surface free energy [5]. More specifically, signal transduction via the piezoelectric mechanism operates well in complex, often optically-intractable media. We demonstrate here that with improvements to acoustic biosensor liquid handling, thermal control, surface chemistries and microfluidics, increases in sensitivity are achieved that enable both high and low molecular weight analytes to be detected. By formation of a non-planar three-dimensional matrix to which a member of a specific binding pair can be attached, an increased amount of the other member of the pair can be captured. This not only increases receptor binding capacity and sensitivity, but also has the effect of reducing the degree of non-specific binding to the surface by effectively masking the chemical and physical properties of the metallic electrode surface. The technology can thus be applied to an extremely wide range of biological and chemical entities with a molecular weight range from less than 200 Daltons through to an entire bacterium or cell.

II. EXPERIMENTAL

A. Materials

Dextran T70, T500 and NAP5 gel filtration columns were from GE Healthcare, UK. Sodium chloroacetate, phosphate buffered saline pH 7.4 (PBS), bovine serum albumin (BSA), ethanolamine, Tween 20, Trizma hydrochloride, Trizma base, D-biotin, 4-carboxybenzenesulfonamide (CBS), benzenesulfonamide, sulfanilamide, dansylamide and human carbonic anhydrase isoform II (hCAII) were from Sigma-Aldrich. Ethyl-3(3-dimethyl amino) propyl carbodiimide-HCl salt (EDC·HCl) and N-hydroxyl succinimide (NHS) were from Pierce Biotechnology, Inc. IgG fraction monoclonal mouse anti-biotin and ChromPure mouse IgG whole molecule were from Jackson ImmunoResearch Laboratory, Inc. Heat-inactivated *E. coli* O157:H7 cells were obtained from Kirkegaard and Perry Laboratory (KPL). Five clinical *E. coli* isolates were provided by Dr Derek Brown (Addenbrookes, Cambridge, UK) and an ATCC *E. coli* 25922 were used as negative controls. Five of these isolates were live bacteria, with heat-inactivated *E. coli* 170044 being used as a killed control. Affinity purified goat anti-O157 polyclonal antibodies (pAbs) were obtained from KPL. Anti-O157 pAbs were isolated from a pooled serum from goats immunised with heat-killed whole cells of *E. coli* O157:H7. The lyophilised anti-O157 antibody was reconstituted with 0.3 M sodium phosphate buffer (0.1 M NaH_2PO_4, 0.2 M Na_2HPO_4), pH 7.4 to a concentration of 10 mg/mL and then further diluted to 1 mg/mL with phosphate-buffered saline (PBS), pH 7.4.

B. Preparation of derivatised polymers and sensor surfaces

Preparation of 2-(pyridinyldithio)ethaneamine (PDEA), 4-nitrophenyl carbonated dextran, 2-(pyridinyldithio)ethyl carbamoyl dextran (PDEC dextran), carboxymethylated dextran T500 (CMD-T500), coating onto sensor surfaces and stability testing were carried out as described in the literature [6, 7].

C. RAP Instrumentation and Sensors

RAP experiments [6] were conducted using a manually operated or automated two-channel RAP platform, or a fully-automated four-channel RAP•*id* platform (TTP LabTech Ltd). The instruments apply the principles of QCM, in that a high frequency (16.5 MHz) voltage is applied to a piezo-electric quartz crystal to induce the crystal to oscillate, and its resonant frequency is then monitored in real time. The two-channel instruments comprised a pair of oscillating crystal sensors mounted in parallel micro-fluidic flow cells, allowing sample to flow across two surfaces simultaneously. As sample was flowed across 'control' and 'active' sensors, binding to the 'active' sensor was measured as a change in the resonant frequency, with the 'control' sensor acting as a subtractive reference. Four-channel instruments comprised a duplication of the two-channel system, with two pairs of oscillating sensors and flow cells.

The RAP instruments (Fig. 1) were fitted with a thermally-stable sensor mounting block providing temperature control at 25°C, with microfluidic and electrical connections to the pairs of piezo-electric sensors. Buffer flow was maintained throughout all experiments with two syringe pumps under software control. Microfluidics comprised separate flow-paths to individual flow cells, as well as a common flow path split to address both flow cells simultaneously. Interchange between the different flow paths was controlled by pneumatically-operated valves. Sensors comprised standard quartz wafers evaporation-deposited with gold electrodes. Sensors were coated with a planar carboxylic acid-terminated linker layer to provide a surface for protein immobilisation, or a high capacity carboxymethylated dextran T500 (CMD-T500) polymer surface [6], then mounted in an acrylic cassette (TTP LabTech Ltd). Mouse monoclonal anti-biotin and mouse IgG antibodies were prepared at 50 µg/mL in 10 mM phosphate buffer, pH 6.5. CMD-T500 polymer-coated

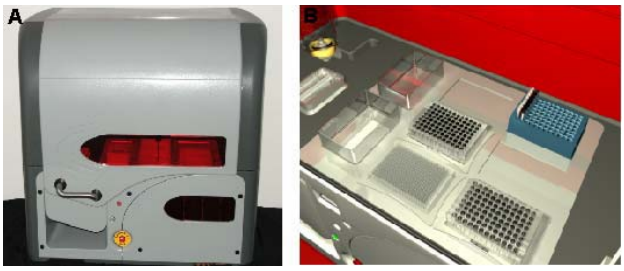

Figure 1. A) The RAP•*id* 4 system and B) temperature controlled bed layout, with capacity for up to 8 microtiter plates, a wash station, a bulk reagent reservoir and separate injection ports for each flow cell.

sensor surfaces were activated with EDC-NHS at 10 µL/min/channel for 5 min. Mouse anti-biotin or mouse IgG antibodies were then flowed cross the activated CMD-T500 surfaces at 25 µL/min/channel for 5 min. Both sensor surfaces were then treated with 1 M ethanolamine pH 8.5 solution at 25 µL/min/channel for 5 min to cap any unreacted NHS ester groups.

D. Biotin binding assay

Biotin binding assays were carried out using PBS pH 7.4 as the running buffer at 25 µL/min/channel flow rate. D-biotin, D-glucose (a neutral, small molecule, non-binding control), and 4-carboxybenzenesulfonamide (a charged, small molecule, non-binding control) were prepared as 1 mM stock solutions in PBS; stock solutions were then diluted to 10 µM in PBS and applied to both anti-biotin antibody 'active' surface and mouse IgG antibody 'control' surface for 1 min, then allowed to dissociate under PBS running buffer flow. PBS was applied as a blank vehicle control. All samples were tested in duplicate. The mouse IgG antibody immobilised 'control' flow cell responses were subtracted from the anti-biotin antibody immobilised 'active' flow cell responses to normalise for any minor bulk shift between running buffer and sample buffer. All control-subtracted binding responses were then superimposed and aligned to the start of the drug injection. The response to a blank PBS injection was then subtracted from each drug response. Duplicate concentrations of D-biotin in 3-fold dilutions from 10 µM to 4.56 nM were applied to both anti-biotin antibody 'active' surface and mouse IgG 'control' surface for 1 min then allowed to dissociate under PBS running buffer flow. Data were then processed as above. Mean binding responses over the interval from 25 sec to 60 sec during the sample injection were used to plot the equilibrium binding curve, and fitted to the Michaelis-Menten equation.

E. Carbonic Anhydrase

For RAP assays, sensor surfaces were immobilized with hCAII by first activating the CMD-T500 polymer coating with EDC-NHS at 12.5 µL/min/channel for 7 min. hCAII was prepared at 100 µg/mL in 10 mM sodium acetate buffer, pH 5.0 and applied to one flow cell of a dual sensor cassette at the same flow rate for 7 min; the second flow cell of the dual sensor cassette was treated with 10 mM acetate buffer, pH 5.0. Both sensor surfaces were then treated with 1 M ethanolamine solution, pH 8.5, at the same flow rate for 7 min to cap any unreacted NHS ester groups. 4-carboxybenzenesulfonamide, benzenesulfonamide, sulfanilamide (all hCAII binding small molecule compounds) and glucose (a non-binding small molecule control at hCAII) were prepared as 10 mM stock solutions in PBS; stock solutions were then diluted to 25 µM in PBS. All hCAII binding assays were carried out using PBS pH 7.4 as the running buffer, with sample / buffer flow rate maintained at 25 µl/min/channel throughout. Compounds at 25 µM in PBS were applied to 'control' (activated-capped) and hCAII-immobilised 'active' sensor surfaces for 1 min, then allowed to dissociate under PBS running buffer flow. PBS was applied as a blank vehicle control. All samples were tested in duplicate. The 'control' flow cell responses were subtracted from the hCAII immobilised 'active' flow cell responses to normalise for any minor bulk shift between running buffer and sample buffer. All control-subtracted binding responses were then superimposed and aligned to the start of the drug injection. The response to a blank PBS injection was then subtracted from each drug response.

For concentration-response relationships, duplicate concentrations of CBS in 2-fold dilutions from 25 µM to 780 nM were flowed across hCAII-immobilised and control sensor surfaces at 25 µL/min/channel for 1 min, then allowed to dissociate under PBS running buffer flow. Data were processed as above. The compiled, control-subtracted, blank subtracted CBS binding responses were then fitted to a global 1:1 Langmuir binding model. Mean binding responses over the interval from 30 sec to 60 sec during the sample injection were also used to plot the equilibrium binding curve.

Dansylamide was prepared as a 10 mM stock solution in dimethylsulfoxide (DMSO); the stock solution was then diluted to 100 µM in PBS to give an intermediate solution containing 1% DMSO. Further dilutions to 25 µM, and 2-fold serial dilutions to 780 nM, were made using PBS with 1% DMSO in order to maintain the same DMSO concentration throughout the series. Running buffer used was PBS with 1% DMSO. Dansylamide samples were then flowed across the 'active' and 'control' sensor surfaces as described for CBS. PBS + 1% DMSO was used as a buffer blank. Kinetic binding data were processed as described for CBS.

F. E. Coli 0157:H7

Sensor surfaces were prepared before exposure to bacteria binding by immobilising anti-O157 pAbs onto the 'sample' sensor surface and mouse IgG onto the 'control' sensor surface using conventional amine coupling chemistry. Sensor surfaces were activated with a 1:1 mixture of 400 mM EDC and 100 mM NHS, prepared in 0.22 µm-filtered deionised water, and mixed immediately prior to use (final concentrations; 200 mM EDC and 50 mM NHS). This mixture was injected simultaneously across four sensor surfaces for 3 min at a flow rate of 25 µL/min. Antibodies were prepared for immobilisation at 50 µg/mL in immobilisation buffer comprising 10 mM sodium acetate, pH 4.5, and were injected simultaneously across separate sensor surfaces for 3 min at a flow rate of 25 µL/min. Non-reacted NHS esters were then capped with 1 M ethanolamine prepared in 0.22 µm filtered deionised water, pH 8.5. Running buffer between sample injections was HEPES-buffered saline (HBS), pH 7.4, containing 10 mM HEPES, 150 mM NaCl, 3.4 mM EDTA, 0.005% Tween 20, pH 7.4, at a flow rate of 25 µL/min.

Binding interactions between *E. coli* O157:H7 and antibodies were monitored in real-time. Both direct binding (bacteria

only) and sandwich assays (bacteria followed by further antibody) were constructed for detection of *E. coli* O157:H7 using anti-O157 antibodies covalently attached onto activated sensors. The binding signal was quantified as the level of frequency change at the end of the contact time with the sample. Non-specific binding was assayed by passing different *E. coli* controls over the anti-O157 antibody immobilized sensor. To investigate the assay sensitivity pre-reconstituted *E. coli* O157:H7 and *E. coli* 170044 control samples were used. As these reconstituted samples had been stored at -80°C for over one year, a centrifugation step (10 s at 2400 g) was performed to remove large particulate aggregates. The supernatants after centrifugation were then reserved for RAP assay experiment. A sample of each supernatant was Gram stained and counted using a Haemocytometer to give a stock concentration level (bacteria/mL).

III. Results and Discussion

A. Small molecule detection

To determine the binding selectivity of the RAP sensor surfaces, 10 µM D-biotin solution in PBS pH 7.4, or PBS pH 7.4 blank, were flowed over anti-biotin antibody- and mouse IgG antibody-coated surfaces. A 39 Hz binding response was elicited by 10 µM D-biotin on the anti-biotin antibody surface (Fig. 2A, ▲) but no binding response (< 1 Hz) on the mouse IgG antibody surface (Fig. 2A, ×). PBS blank injections elicited no response (< 1 Hz) on either surface (Fig. 2A, ○ and □). To determine the binding specificity of the anti-biotin surface, 10 µM solutions in PBS, pH 7.4, of D-biotin (244 Da), D-glucose (180 Da; used as a neutral non-binding control), CBS (201 Da; used as a charged, non-anti-biotin-antibody binding control) and PBS blank were applied in turn to both the anti-biotin antibody active surface and the mouse IgG antibody control surface. As before, 10 µM D-biotin elicited a 39 Hz response on the anti-biotin antibody surface (Fig. 2B, ▲), but glucose (Fig. 2B, ×) and CBS (Fig. 2B, ○) did not give a response.

To determine the affinity of the anti-biotin antibody surface for D-biotin, 3-fold dilutions of D-biotin from 10 µM to 4.56 nM were then flowed sequentially across both surfaces and allowed to bind to the anti-biotin antibody, and then to dissociate under continuous running buffer flow. A correction for the minor bulk shift between the running buffer and the sample buffer was made by subtracting the responses on the mouse IgG control flow cell from the responses on the anti-biotin antibody active flow cell. The response to a blank PBS injection was also subtracted from each D-biotin binding response. The D-biotin binding responses were superimposed and aligned to the start of the sample injection (Fig. 2C), then fitted to a global 1:1 Langmuir binding model, giving a K_D of 340 nM. The mean equilibrium binding amplitudes for each biotin concentration were also plotted against the logarithm of biotin concentration (Fig. 2D), and the data fitted to the Michaelis-Menten equilibrium binding equation to give a K_D of 300 nM. Thus, RAP binding response data can be used to calculate binding affinity using either a kinetic fit model (measuring binding association and dissociation rates to calculate K_D) or an equilibrium binding model, with a high degree of congruence.

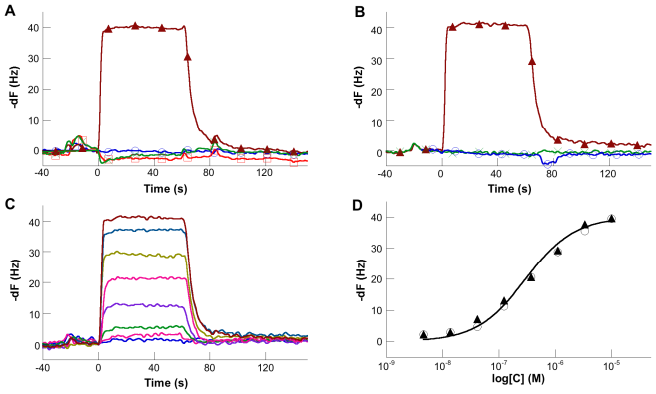

Figure 2. Biotin binding to anti-biotin antibody immobilised onto a CMD-T500 sensor surface. **A:** Comparison of biotin binding signal with blank and control signals: PBS blank on anti-biotin antibody surface (○); PBS blank on mouse IgG control surface (□); 10 µM biotin on anti-biotin antibody surface (▲); 10 µM biotin on mouse IgG control surface (×). Binding is only observed with D-biotin on the anti-biotin antibody surface. **B:** Specificity of binding responses for biotin (▲); CBS (○) and glucose (×). Only D-biotin binds to mouse anti-biotin antibody; CBS and glucose do not bind. **C:** Binding responses for a series of 3-fold dilutions of biotin in PBS from 10 µM to 4.56 nM. **D:** The biotin equilibrium binding response amplitude for each biotin concentration (tested in duplicate) plotted against the logarithm of biotin concentration (duplicates: ▲ and ○), with the sigmoidal equilibrium binding curve fitted by the Michaelis-Menten equation superimposed. The equilibrium binding K_D was calculated as 300 nM.

B. Carbonic anhydrase

Carbonic anhydrase (CA) is ubiquitously expressed, with 14 isoforms identified in vertebrates. CA I, II, III and VII are cytoplasmic, all convert carbon dioxide and water to bicarbonate. CA is also involved in other carbon dioxide-dependent processes, e.g. bone calcification and resorption, and tumorigenicity. Since the discovery of the potent antibacterial activity of sulfanilamide in 1935, medicinal chemists have investigated sulfonamides as a potential source of therapeutic agents. Sulfonamide-based CA inhibitors are widely used today as pharmacological agents for the treatment or prevention of a variety of diseases including glaucoma, cystoid macular oedema, diabetic retinopathy, epilepsy and a variety of neurological and neuromuscular disorders [8]. Inhibitor-CA interactions are thus a suitable pharmacologically relevant system for novel screening platforms. In addition, published data describing interaction affinities and kinetics for sulfonamide-CA interactions obtained using isothermal titration calorimetry and stopped-flow fluorescence are available [9]. The enzyme is also well characterised and is known to form a 1:1 complex with sulfonamides.

Human carbonic anhydrase isoform II (hCAII) was immobilised onto CMD-T500 coated sensors using EDC-NHS coupling chemistry, as described earlier. Rather than

use BSA immobilisation onto the second sensor surface as a non-binding control, the second surface was simply activated with EDC-NHS and then capped with ethanolamine. This method resulted in approximately 2500 to 3200 Hz of hCAII immobilized onto the CMD-T500 active sensor surface. In contrast, only 215 ± 60 Hz (mean ± S.D., n = 4) of hCAII were immobilized onto a planar, carboxylic acid-terminated linker layer.

For drug binding to hCAII immobilized onto CMD-T500 polymer coated sensors, duplicate 25 µM injections of the sulfonamide hCAII inhibitors: CBS, benzenesulfonamide and sulfanilamide were passed across hCAII and control surfaces for 1 min, followed by dissociation under running buffer flow. These gave binding responses with different amplitudes for each inhibitor. Injections of the hCAII non-binding control, D-glucose, did not give binding responses (< 1 Hz). All binding responses had reverted to baseline levels within a minute of washing off the drug sample with running buffer flow, showing that dissociation was rapid. From the magnitude of the binding response for the different compounds, a rapid estimate of the rank order of binding levels could be made: CBS > sulfanilamide >= benzenesulfonamide >>> glucose, consistent with the known rank order of hCAII inhibition by these compounds [8, 10].

To determine the binding affinity for CBS, serial 2-fold dilutions were prepared in PBS and passed over the sensor surfaces, in duplicate, as described above. Binding responses were control subtracted, aligned to the start of the drug injection, and then blank subtracted. A global 1:1 Langmuir binding model was fitted to the response curves to determine the binding association and dissociation rates, from which the kinetic fit binding affinity (K_D) was calculated as 2.6 µM. The mean binding response amplitudes at each of the CBS concentrations were also determined and plotted against the logarithm of the CBS concentration. Fitting these data to the Michaelis-Menten equation gave an equilibrium binding K_D of 2.2 µM. This value is in close accordance with the value obtained by kinetic analysis. The results of independent repetitions of this affinity analysis for CBS, and for the structurally distinct hCAII inhibitor, dansylamide, are summarized in Table 1.

TABLE I. COMPARISON OF AFFINITY INTERACTION CONSTANTSFOR HCAII/SULFONAMIDE INTERACTIONS

Analysis Method[a]	Compound	K_D (nM)	Ref.
RAP (n=5)	CBS	2670 ± 1600	This work
ITC (n=5)	CBS	730 ± 20	[9]
RAP (n=3)	DNSA	1260 ± 990	This work
ITC (n=2)	DNSA	360 ± 40	[9]
SFF (n=4)	DNSA	420 ± 100	[9]

a. ITC: Isothermal Titration Calorimetry; SFF: Stopped Flow Fluorescence

C. Bacteria Detection

In order to challenge the molecular weight dynamic range and sensitivity of the system, we also developed an automated, rapid (< 20 min.), and label-free testing protocol for detection of *E. coli* O157:H7 (O157) [11]. This pathogen is a rare serotype of *E. coli* that produces large quantities of a powerful toxin causing severe damage to the lining of the intestine. It can induce severe diarrhoea, hemorrhagic colitis and kidney damage. People are commonly infected by consuming contaminated food or water, as bacteria can live asymptomatically in healthy ruminant mammals and meats can become contaminated during processing [12, 13]. A rapid test to identify contaminated foodstuffs, water supplies or infected persons would assist in reducing the risk of spreading of this disease. Both direct and sandwich RAP immunoassays were constructed for detection of *E. coli* O157:H7. Anti-O157 specific polyclonal antibodies were immobilized onto an activated acoustic sensor via carbodiimide coupling chemistry. *E. coli* O157:H7 either from whole cell suspension or from supernatants prepared by a brief centrifugation, were passed over immobilized antibodies and the binding signal was then enhanced by subsequent exposure to further anti-O157 antibodies in a sandwich assay. Five clinical *E. coli* isolates and an ATCC strain were evaluated as negative controls.

Six dilutions of *E. coli* O157:H7 supernatant (20, 60 and then log-fold to 600,000 bacteria/mL) were injected onto anti-O157 immobilised sensors. The signals generated by either direct binding or sandwich assay decreased with increasing the dilution of *E. coli* O157:H7 in analysed samples. The minimum measurable resonant change was found to be 6000 bacteria/mL for direct O157 binding and 600 bacteria/mL for the sandwich assay. Non-specific binding for both assay formats was determined by passing *E. coli* controls (170044 at 600,000 bacteria/mL and other live bacteria at 10^7 bacteria/mL) over the anti-O157 immobilized sensor.

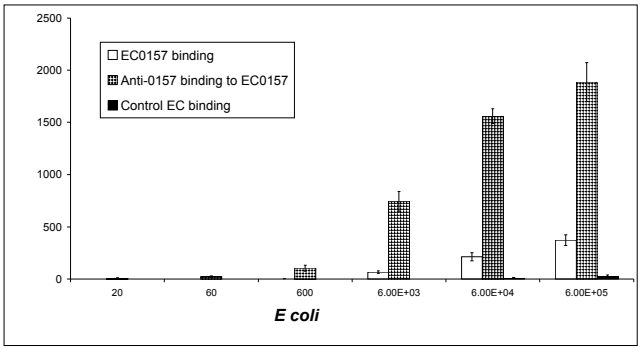

Figure 3. Binding levels for specific signal from *E. coli* O157:H7 from various dilutions (CFU/mL) using the direct assay (white open), the sandwich assay (striped grey), with associated average responses for five different control strains of *E. coli* (solid black); error bars are S.D.; n = 5.

The sandwich assay was approximately 100-fold more sensitive than the direct assay with a high specificity for *E. coli* O157:H7 over *E. coli* controls (Fig. 3). *E. coli* O157:H7 at 60 bacteria/mL was detected when a supernatant from centrifuged *E. coli* O157:H7 sample was used. Horse serum and human urine were spiked with whole cell suspensions of *E. coli* O157:H7 and *E. coli* 170044 control.

The potential clinical utility of the assay was further explored using whole cell suspensions of freshly reconstituted *E. coli* O157:H7 and freshly thawed *E. coli* 170044. These bacterial suspensions were Gram-stained, counted using a Haemocytometer and then spiked at a concentration 10^7 bacteria/mL into undiluted horse serum, human urine or HBS buffer. They were then analysed by direct binding and sandwich assay following the same method as described earlier. This preliminary study showed that *E. coli* O157:H7 was clearly detectable in undiluted matrix with negligible signal for the *E. coli* 170044 control. The signal for O157 in serum was reduced compared to the result in buffer by approximately 85% for the direct binding assay and by 80% for the sandwich assay, but was substantially unaffected by urine. The latter sample matrix resulted in a signal level within 10% of that obtained in buffer. The level of non-specific binding with the *E. coli* 170044 control strain spiked in serum or urine was similar to that found in buffer, suggesting that the undiluted complex matrices did not contribute significantly to the amount of non-specific binding.

IV. CONCLUSION

Examples of robust small molecule sensing using acoustic wave devices in the literature are rare due to the significant demands on system sensitivity for low mass detection. We have shown using a soluble receptor that enzymes can be readily coupled to dextran-based sensor surfaces via amine or alternative chemistries, and small molecule (drug candidate) binding detected. For high molecular weight analytes, preliminary data for bacterial detection showed that anti-O157 binding to *E. coli* O157:H7 was clearly discernable in undiluted matrix at a high level of specificity and sensitivity. The advantages of this assay were automation, short analysis time with real time reporting, simple testing protocols, real, and high specificity.

It is thus possible to exploit thickness shear mode quartz resonators in the detection and characterization of interactions between ligands, analytes and receptors with a wide range of biological and chemical entities; from those with a molecular weight of less than 200 Daltons through to an entire bacterium.

ACKNOWLEDGMENT

We gratefully acknowledge the work and original contributions of Dr. Kevin Thompson and Dr. Ling Huang, and Dr. Derek Brown from Addenbrookes Hospital, Cambridge, U.K. for provision of the clinical bacterial isolates.

REFERENCES

[1] G. Sauerbrey, "Verwendung von Schwingquarzen zur Wagung dunner Schichten und zur Microwagang," *Z. Phys.*, vol. 155, pp. 206-212, 1959.

[2] T. Nomura and M. Okuhara, "Frequency-shifts of piezoelectric quartz crystals immersed in organic liquids," *Anal. Chim. Acta*, vol. 142, pp. 281-284, 1982.

[3] K. K. Kanazawa, "Mechanical behaviour of films on the quartz microbalance," *Faraday Discussions*, pp. 77-90, 1997.

[4] A. Janshoff, H. J. Galla, and C. Steinem, "Piezoelectric mass-sensing devices as biosensors - An alternative to optical biosensors?," *Angewandte Chemie-International Edition*, vol. 39, pp. 4004-4032, 2000.

[5] K. A. Marx, "Quartz crystal microbalance: a useful tool for studying thin polymer films and complex biomolecular systems at the solution-surface interface," *Biomacromolecules*, vol. 4, pp. 1099-120, 2003.

[6] X. Li, K. S. Thompson, B. Godber, and M. A. Cooper, "Quantification of small molecule-receptor affinities and kinetics by acoustic profiling," *Assay Drug Dev Technol*, vol. 4, pp. 565-73, 2006.

[7] X. Li, C. Abell, and M. A. Cooper, "Single step biocompatible coating for thiol coupling of receptors via 2-(pyridinyldithio)ethylcarbamoyl dextran, 2008, 61, 113–117.," *Colloid Interfac. Sci. B.*, vol. 61, pp. 113-117, 2008.

[8] S. Zimmerman, A. Innocenti, A. Casini, J. G. Ferry, A. Scozzafava, and C. T. Supuran, "Carbonic anhydrase inhibitors. Inhibition of the prokaryotic beta and gamma-class enzymes from Archaea with sulfonamides," *Bioorg Med Chem Lett*, vol. 14, pp. 6001-6, 2004.

[9] Y. S. Day, C. L. Baird, R. L. Rich, and D. G. Myszka, "Direct comparison of binding equilibrium, thermodynamic, and rate constants determined by surface- and solution-based biophysical methods," *Protein Sci*, vol. 11, pp. 1017-25, 2002.

[10] S. A. Poulsen, L. F. Bornaghi, and P. C. Healy, "Synthesis and structure-activity relationships of novel benzene sulfonamides with potent binding affinity for bovine carbonic anhydrase II.," *Bioorg Med Chem Lett*, vol. 15, pp. 5429-5433, 2006.

[11] L. Huang and M. A. Cooper, "Real-time label-free acoustic technology for rapid detection of Escherichia coli O157:H7," *Clin Chem*, vol. 52, pp. 2148-51, 2006.

[12] R. L. Buchanan and M. P. Doyle, "Foodborne disease significance of Escherichia coli O157:H7 and other enterohemorrhagic E-coli," *Food Technol*, vol. 51, pp. 69-76, 1997.

[13] R. E. Besser, P. M. Griffin, and L. Slutsker, "Escherichia coli O157 : H7 gastroenteritis and the hemolytic uremic syndrome: An emerging infectious disease," *Annu Rev Med*, vol. 50, pp. 355-367, 1999.